

Supplement of Biogeosciences, 15, 2361–2378, 2018
<https://doi.org/10.5194/bg-15-2361-2018-supplement>
© Author(s) 2018. This work is distributed under
the Creative Commons Attribution 4.0 License.



Supplement of

Interannual drivers of the seasonal cycle of CO₂ in the Southern Ocean

Luke Gregor et al.

Correspondence to: Luke Gregor (luke.gregor@uct.ac.za)

The copyright of individual parts of the supplement might differ from the CC BY 4.0 License.

S Supplementary Materials

S1 Wind speed and regional surface area

The regional magnitude of integrated air-sea CO₂ fluxes are in part determined by the wind speed and surface area of the specific region. Figure S1a shows the average wind speeds for summer and winter for each of the regions as defined in Figure 1. The wind product used is CCMP v2 (Atlas et al., 2011). Figure S1b shows the surface area of each of the regions. Note that the Indian sector of the PFZ has both the highest average wind speed and has the largest surface area. This explains the dominance of the region in the determination of interannual variability of F_{CO_2} (Figure S4), even though ΔpCO_2 (Figure 4) variability is relatively weak.

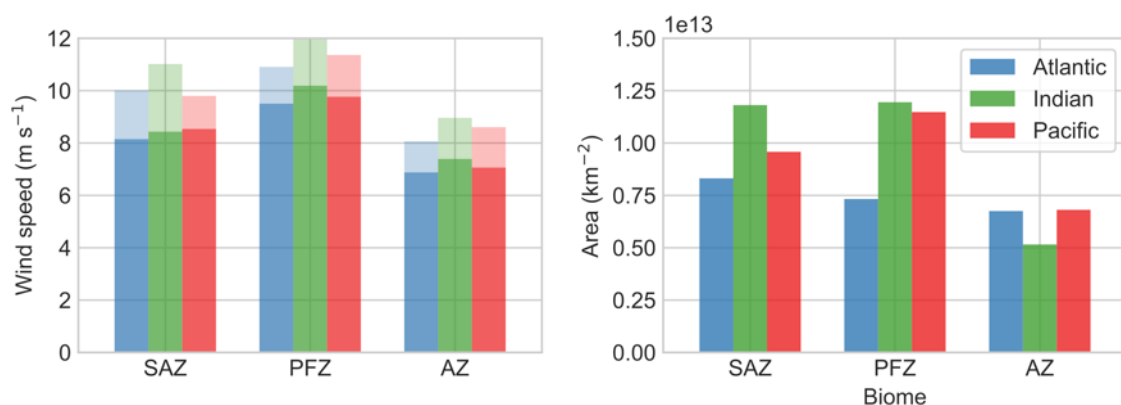


Figure S1: (a) Average wind speeds for each of the biomes for summer (dark) and winter (light). The ocean basins are shown by the colours depicted in the key for (b), which shows the size of each region separated by biome and basin.

S2 Seasonal time series

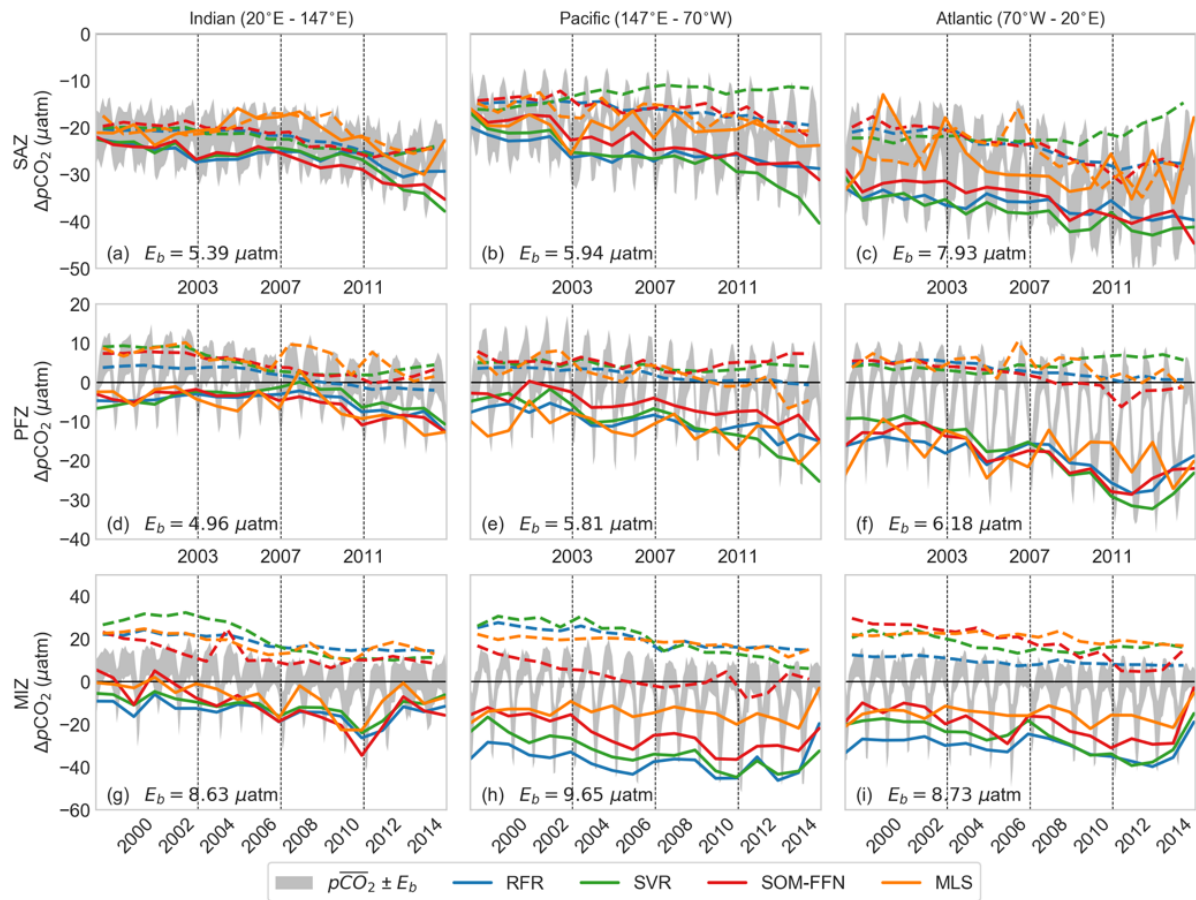


Figure S2: The regional breakdown of the seasonal averages for $\Delta p\text{CO}_2$. The seasonal mean for summer (solid) and winter (dashed) for each method is represented by the different coloured lines as shown in the key, where MLS is the Mixed Layer Scheme. The other methods are as in the main text. The grey fill is the ensemble mean $\Delta p\text{CO}_2 \pm E_b$, where E_b is the between-method error calculated as in Equation 5.

Figure S2 shows the seasonal time series for each region, maintaining separate seasonal averages for each method. We also include the Marginal Ice Zone plots, with all plots showing the average between-method error.

The Mixed Layer Scheme (MLS) method by Rödenbeck et al. (2013) is also included. Note that the MLS is not a machine-learning method as it incorporates prior knowledge of the system. The method results in divergent estimates of $\Delta p\text{CO}_2$, particularly in the SAZ. The MLS fails to produce a seasonal cycle, with winter and summer $\Delta p\text{CO}_2$ having the same magnitude. Further work will have to be done to understand the cause for this difference. We do not include MLS in the main ensemble as we cannot explain this difference. The methods are in much better agreement in the PFZ.

Figure S3 is the same as Figure 4, but as the mean of the entire Southern Ocean (including the MIZ).

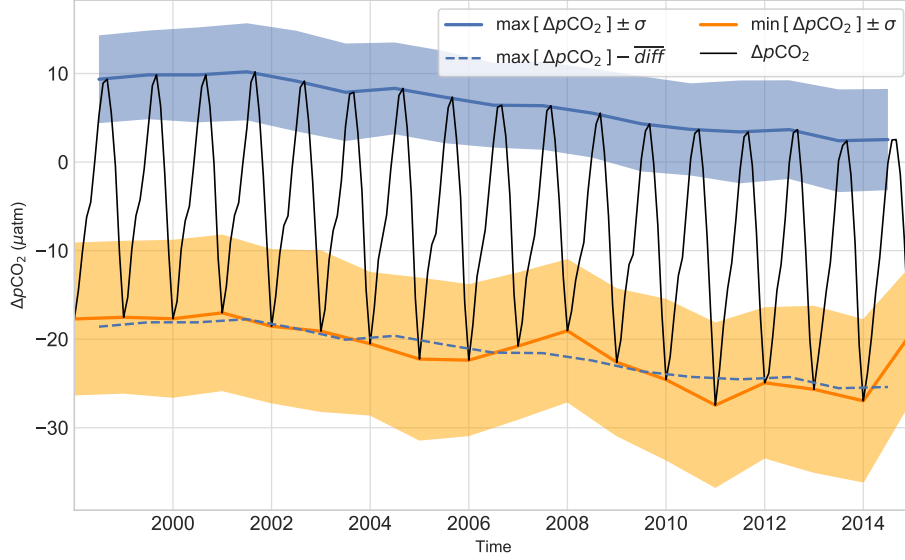


Figure S3: The ensemble mean of $\Delta p\text{CO}_2$ (black) for the entire Southern Ocean (including MIZ). The blue line shows the maximum for each year (winter outgassing) and the dashed blue line shows the same line less the average seasonal amplitude (\overline{diff}) – this is the expected amplitude. The orange line shows the minimum $\Delta p\text{CO}_2$ for each summer season. The shaded regions around the seasonal maxima and minima show the standard deviation of the three products. E_b is the average between-method error and $\Delta p\text{CO}_2$ is the average for the entire time series.

S3 Air-Sea CO₂ Fluxes

Air-sea CO₂ fluxes are calculated with:

$$F_{\text{CO}_2} = k_w \cdot K_0 \cdot (p\text{CO}_2^{\text{sea}} - p\text{CO}_2^{\text{atm}}) \quad (\text{S1})$$

The gas transfer velocity (k_w) is calculated using a quadratic dependency of wind speed with the coefficients of Wanninkhof et al., 2009. Coefficients from Weiss (1974) are used to calculate K_0 and $\Delta p\text{CO}_2$ is estimated by the empirical models. Wind speed is calculated from the u and v vectors ($\sqrt{u^2 + v^2}$) of the Cross-Calibrated Multiplatform Product (CCMP) v2 (Atlas et al., 2011; Wentz et al., 2015). Wind speed is one of the largest contributors to the uncertainty in flux estimates, so the choice of the wind product could have a large impact on flux estimates as well as interpretation of the drivers of CO₂ (Takahashi et al., 2009). We use the ensemble mean $\Delta p\text{CO}_2$ from Figure 4 to calculate fluxes – note that the ensemble mean does not include the MLS shown in Figure S2.

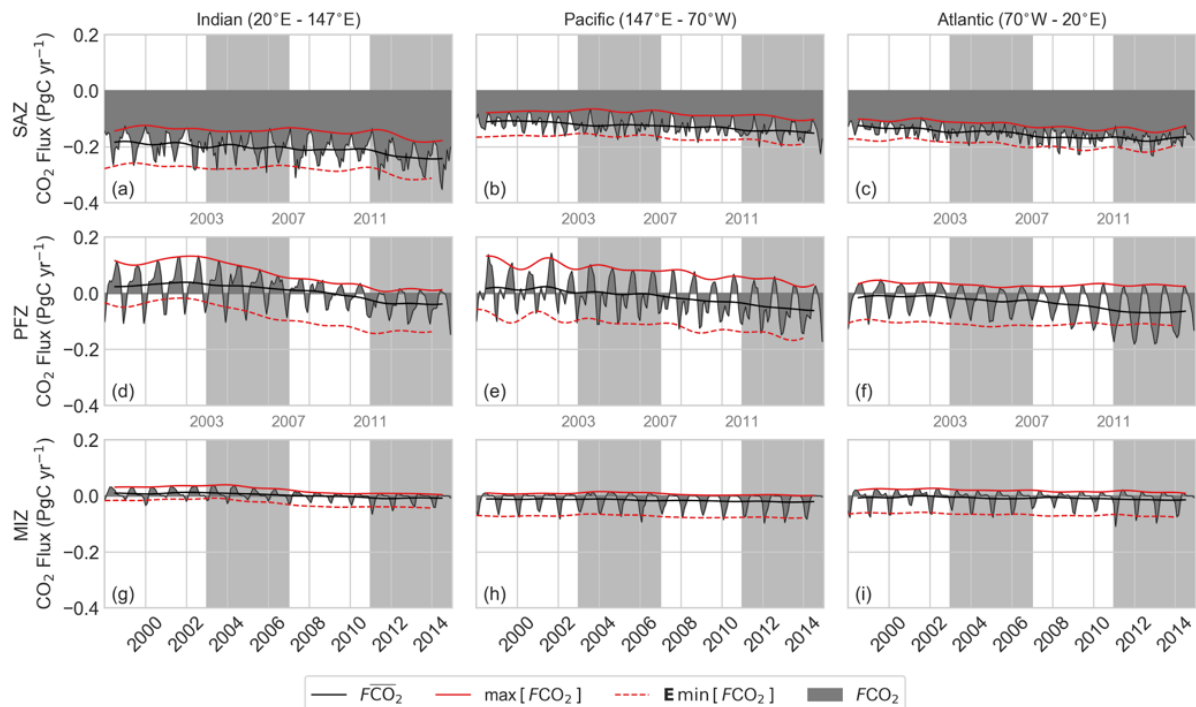


Figure S4: FCO_2 (dark grey) plotted by biome (rows) and basin (columns). Biomes are defined by Fay and McKinley (2014a). The solid red line shows the maximum for each year (winter outgassing) and the dashed line shows the same line less the average difference between the minimum and maximum – this is the expected amplitude. Lighter grey shading in (a-i) shows periods used in Figure 5 and 6. Note that fluxes in the MIZ are calculated from a reduced surface area to maintain consistency between methods.

Mean FCO_2 is shown in Figure S4. Note that the apparent weak fluxes in the MIZ are due to the reduction of the surface area and hence flux to maintain equal weighting between machine-learning methods. The SAZ clearly dominates the annual uptake of CO_2 in the Southern Ocean, but the interannual variability is dominated by the PFZ. An interesting point of the SAZ is that the seasonal cycle of wind speed (strong in winter, weak in summer) opposes that of ΔpCO_2 sink (weak in winter, strong in summer). The net result is that, compared to ΔpCO_2 , the seasonal amplitude of FCO_2 is reduced. The same effect shifts the mean flux in the PFZ, but does not affect the amplitude, where outgassing is amplified in winter and the sink is weaker than if wind speed were constant. Lastly, Figures S4a,d show that the Indian sector of the Southern Ocean dominate both uptake (SAZ) and the interannual variability (PFZ).

S4 Additional driver variables

Here we show additional variables that accompany Figures 6 and 7. Figure S5 shows winter $Chl-a$, u- and v-components of wind, while Figure S6 shows summer MLD, u- and v-components of wind. These variables are not included in the main analyses as they do not contribute significant information to the proxy variables already present (wind stress, SST and MLD/ $Chl-a$). It is interesting to note that the u- and v- components of wind speed

highlight the zonally asymmetric dipole during winter (Figures S5d,e,g,h) and the annular dipole during summer (Figures S6d,e).

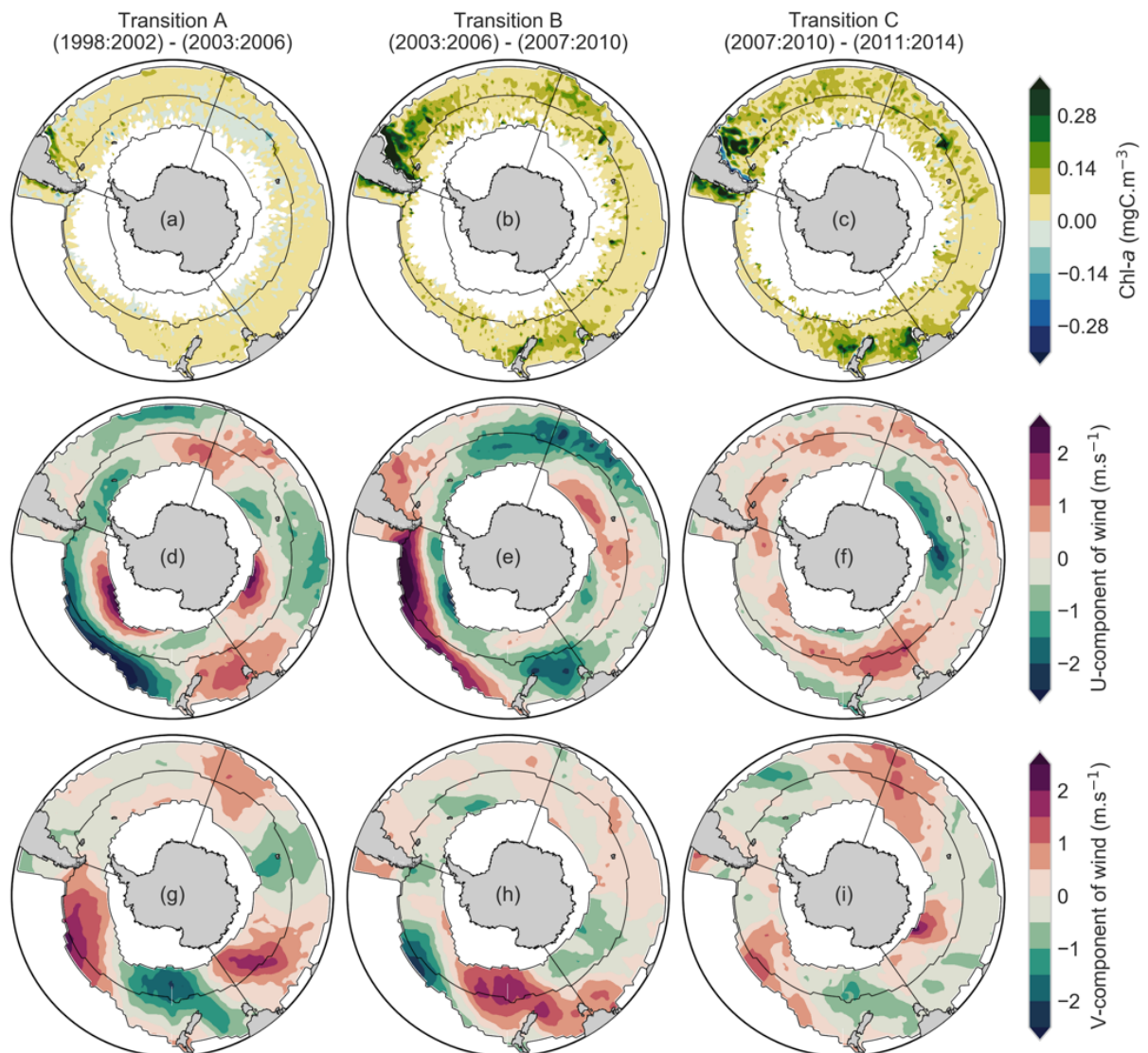


Figure S5: Relative anomalies of winter Chl-*a* (a-c), u- (d-f), and v-components (g-i) of wind for four periods (as shown above each column). The thin black lines show the boundaries for each of the nine regions described by the biomes (Fay and McKinley, 2014a) and basin boundaries.

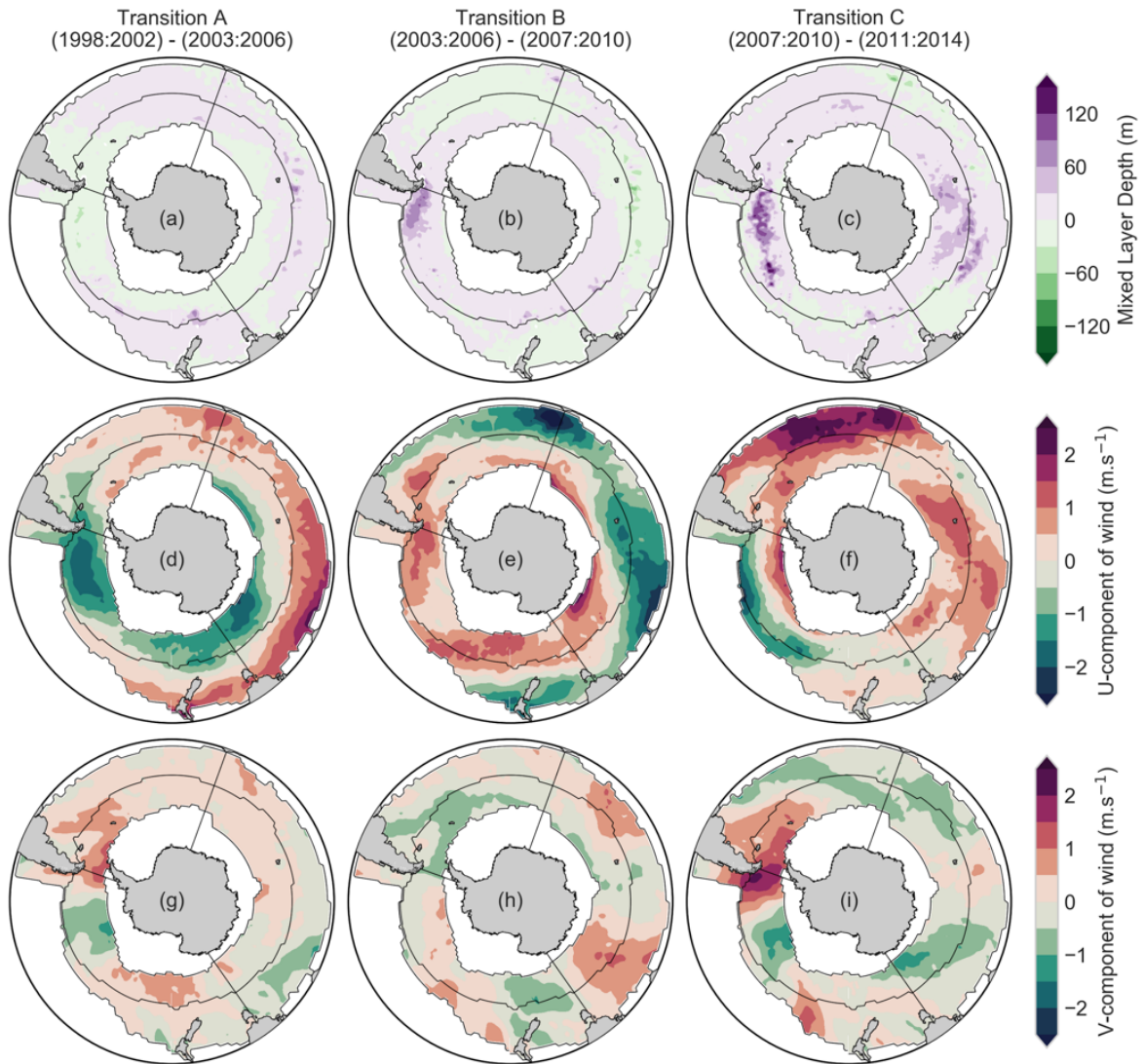


Figure S6: Relative anomalies of summer mixed layer depth (a-c), u- (d-f), and v-components (g-i) of wind for four periods (as shown above each column). The thin black lines show the boundaries for each of the nine regions described by the biomes (Fay and McKinley, 2014a) and basin boundaries.